

line with slope -0.035 and correlation coefficient of 0.999 (Figure 8). These results demonstrate a marked dependence of the Co(III)/Co(II) cathodic peak on pyridine basicity.

Conclusions

Despite the weaker trans influence of chloride compared to the alkyl group, the py ligand in **1** retains its orientation and increases the butterfly bending. The NMR spectral dependence for Costa-type complexes, now assessed with a non-alkyl complex, has the same trends as found for cobaloximes; namely, the Co anisotropy is greater for the Cl than for the alkyl complexes. Furthermore, the results suggest that the shift of the O-H...O signal depends on axial ligand electronic properties more than on Co anisotropy.

The dichloro complex **7** does not undergo solvolysis in CH_3CN but the pyridine/chloro complexes generally are solvolyzed by loss of pyridine. During electrolytic reduction, the weakly ligated Cl in the electrogenerated Co(II) species is available to convert a second Co(III) species to the dichloro complex. Although this behavior complicates the CV profiles, it was possible to obtain the dependence of the Co(III)/Co(II) peak on pyridine basicity. A 260-mV change in the Co(III)/Co(II) cathodic peak was observed when the axial ligand was changed from 4-CNpy to 4-(Me₂N)py.

No similar systematic study of the redox properties of organocobalt analogues has been done. However, for $[\text{CH}_3\text{CNC}(\text{DO})(\text{DOH})\text{pn}]\text{CH}_3^+$ and $[\text{CH}_3\text{CNC}(\text{DO})(\text{DOH})\text{pn}]\text{neo-C}_5\text{H}_{11}^+$ the Co(III)/Co(II) cathodic reduction was found to be -1.42^{16} and -1.37 V,³⁴ respectively, in CH_3CN solvent. The

change is ~ 1.0 V compared to $[\text{CH}_3\text{CNC}(\text{DO})(\text{DOH})\text{pn}]\text{Cl}^+$. Except for these two alkyl Costa-type complexes, the electrochemical properties of the alkyl Costa-type compounds are complex.

Of some interest, the dimethyl analogue of **7** was observed on reduction of $[\text{CH}_3\text{CNC}(\text{DO})(\text{DOH})\text{pn}]\text{CH}_3^+$, indicating some unexpected analogy between the alkyl and the non-alkyl species. However, the Co(II) species produced on reduction of $[\text{CH}_3\text{CNC}(\text{DO})(\text{DOH})\text{pn}]\text{neo-C}_5\text{H}_{11}^+$ is believed to have neopentyl attached to the equatorial ligand.³⁴ Such species have been recently demonstrated in a related system.³⁵ The Co(II)/Co(I) cathodic reduction for $[\text{CH}_3\text{CNC}(\text{DO})(\text{DOH})\text{pn}]\text{neo-C}_5\text{H}_{11}^+$ is -1.4 V, reflecting the change in the equatorial ligand.

Acknowledgment. We are grateful to the National Institutes of Health (Grant GM 29225) for financial support. We also thank Dr. C. L. Hill for the use of the electrochemistry equipment, Dr. P. A. Marzilli for some syntheses, Dr. K. S. Hagen and Dr. M. Sabat for helpful suggestions on the crystallographic study, and Dr. L. Randaccio for communicating unpublished results.

Supplementary Material Available: Tables giving details of the X-ray structural analysis, bond lengths and angles, calculated hydrogen atom coordinates and isotropic thermal parameters, anisotropic thermal parameters, and cyclic voltammetric data for **1-7** at scan rates of $0.1-0.5$ V/s and figures showing a crystal packing diagram and CVs at 0.2 V/s of **1** with addition of py, **1** with addition of chloride, **2, 2** with addition of 4-CNpy, **4, 6** with addition of py, **6** with addition of 2-picoline, $\text{pyCo}(\text{DH})_2\text{Cl}$, and $[(\text{py})_2\text{Co}(\text{DH})_2]\text{PF}_6$ (19 pages); a listing of observed and calculated structure factors (11 pages). Ordering information is given on any current masthead page.

(34) Seeber, R.; Marassi, R.; Parker, W. O., Jr.; Marzilli, L. G. *Organometallics* 1988, 7, 1672.

(35) Daikh, B. E.; Finke, R. G. *J. Am. Chem. Soc.* 1991, 113, 4160.

Contribution from the Department of Chemistry, University of Tsukuba, Tsukuba, Ibaraki 305, Japan

Synthesis and Properties of Cage-Type S-Bridged Co^{III}Zn^{II} Polynuclear Complexes.

Crystal Structure of Spontaneously Resolved $[\{\text{Co}(\text{aet})_3\}_4\text{Zn}_4\text{O}]\text{Br}_6$ (aet = 2-Aminoethanethiolate)

Takumi Konno,* Takayuki Nagashio, Ken-ichi Okamoto, and Jinsai Hidaka

Received July 24, 1991

The reaction of $\text{fac}(\text{S})\text{-}[\text{Co}(\text{aet})_3]$ with ZnBr_2 in water produced a cage-type S-bridge polynuclear complex with a "complete" core $[\text{Zn}_4\text{O}]^{6+}$, $[\{\text{Co}(\text{aet})_3\}_4\text{Zn}_4\text{O}]\text{Br}_6$ (**2**), by way of a precursory cage-type complex with a "defective" core $[\text{Zn}_3\text{Br}]^{5+}$, $[\{\text{Co}(\text{aet})_3\}_4\text{Zn}_3\text{Br}]\text{Br}_5$ (**1**). **2** was subject to spontaneous resolution and its crystal structure and absolute configuration for the (+)₅₈₀ isomer were determined by X-ray crystallography. $[\{\text{Co}(\text{aet})_3\}_4\text{Zn}_4\text{O}]\text{Br}_6 \cdot 9.5\text{H}_2\text{O}$, chemical formula $\text{C}_{24}\text{H}_{91}\text{N}_{12}\text{O}_{10.5}\text{S}_{12}\text{Co}_4\text{Zn}_4\text{Br}_6$, crystallizes in the cubic space group $P2_13$ with $a = 18.981(1)$ Å, $V = 6838.6(3)$ Å³, $Z = 4$, $R = 0.0478$, and $R_w = 0.0448$ for 1844 reflections with $F_o > 5\sigma(F_o)$. The four octahedral $\text{fac}(\text{S})\text{-}[\text{Co}(\text{aet})_3]$ subunits are bound to the tetrahedral $[\text{Zn}_4\text{O}]^{6+}$ core in a tetrahedral arrangement, and each Zn(II) is tetrahedrally coordinated by three thiolato sulfur atoms from three different $\text{fac}(\text{S})\text{-}[\text{Co}(\text{aet})_3]$ subunits and a central μ_4 -oxygen atom. For the (+)₅₈₀ isomer, chiral configurations are regulated to Δ for all four $\text{fac}(\text{S})\text{-}[\text{Co}(\text{aet})_3]$ subunits and R for all 12 bridging sulfur atoms, giving an approximate T symmetrical structure. Cyclic voltammetric measurements in water exhibited four consecutive quasi-reversible redox couples in the region of -0.3 to -0.9 V (vs Ag/AgCl) for **2**, which correspond to the four Co(III)/Co(II) redox reactions, while **1** exhibited four nonreversible reduction waves in the same potential region. The electronic absorption and circular dichroism (CD) spectral behavior of these complexes are discussed in comparison with those of related mononuclear and linear-type S-bridged trinuclear complexes.

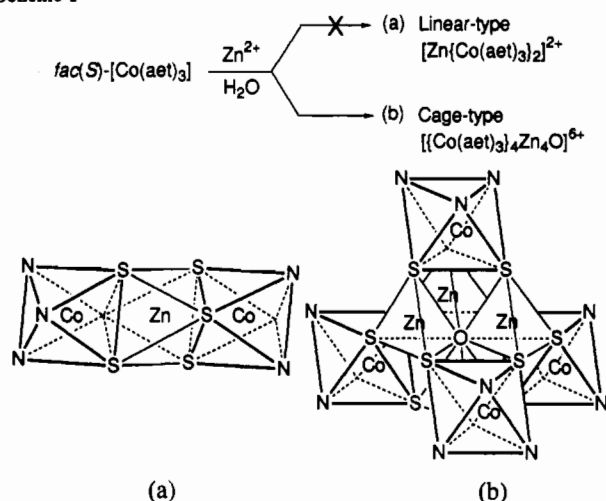
Introduction

One of the most attractive properties of coordinated thiolato ligands is their ability to react readily with a variety of metal ions to form S-bridged polynuclear complexes. For example, a large number of S-bridged polynuclear complexes with 2-aminoethanethiolate (aet, $\text{NH}_2\text{CH}_2\text{CH}_2\text{S}^-$) or L-cysteinate (L-cys, $\text{NH}_2\text{CH}(\text{COO}^-)\text{CH}_2\text{S}^-$) have been prepared using $\text{fac}(\text{S})\text{-}[\text{M}(\text{aet})_3]$ or $\text{fac}(\text{S})\text{-}[\text{M}(\text{L-cys-N}_i\text{S})_3]^{3-}$ ($\text{M} = \text{Co(III)}, \text{Rh(III)}, \text{Ir(III)}$) as the starting complexes.¹⁻⁵ It has been recognized that

these mononuclear complexes function as tridentate ligands to metal ions such as $\text{M}' = \text{Fe(III)}, \text{Co(III)},$ and Ni(II) , which prefer

- (1) (a) Bush, D. H.; Jicha, D. C. *Inorg. Chem.* 1962, 1, 884. (b) Brubaker, G. R.; Douglas, B. E. *Inorg. Chem.* 1967, 6, 1562. (c) DeSimone, R. E.; Ontko, T.; Wardman, L.; Blinn, E. L. *Inorg. Chem.* 1975, 14, 1313. (d) Blinn, E. L.; Butler, P.; Chapman, K. M.; Harris, S. *Inorg. Chim. Acta* 1977, 24, 139. (e) Heeg, M. J.; Blinn, E. L.; Deutsch, E. *Inorg. Chem.* 1985, 24, 1118. (f) Johnson, D. W.; Brewer, T. R. *Inorg. Chim. Acta* 1988, 154, 221.

Scheme I



to take an octahedral geometry, forming linear-type S-bridged trinuclear complexes, $[M'\{M(\text{aet or L-cys-N,S})_3\}_2]^{n+}$ or $n-1$.² The $\text{fac}(\text{S})$ - $[M(\text{aet or L-cys-N,S})_3]^{0 \text{ or } 3-}$ complexes also react with $M'' = \text{Zn}(\text{II})$ and $\text{Cd}(\text{II})$, but none of the reaction products containing tetrahedrally oriented M'' have long been structurally characterized, although the reaction product from $\text{fac}(\text{S})$ - $[\text{Co}(\text{aet})_3]$ and Zn^{2+} has been tentatively assigned as the linear-type S-bridged trinuclear or tetranuclear complex.^{1b,d} We have recently found that the reactions of $\text{fac}(\text{S})$ - $[\text{Rh}(\text{aet})_3]$ with Zn^{2+} or with Cd^{2+} give a new class of cage-type S-bridged polynuclear complexes, $[\{\text{Rh}(\text{aet})_3\}_4M''_4O]^{4+}$, where each M'' is tetrahedrally coordinated by three sulfur atoms from three different $\text{fac}(\text{S})$ - $[\text{Rh}(\text{aet})_3]$ subunits and a central oxygen atom. Furthermore, it was found that the linear-type trinuclear structure in $[\text{Co}^{\text{III}}\{M(\text{aet})_3\}_2]^{3+}$ ($M = \text{Rh}(\text{III}), \text{Ir}(\text{III})$) is convertible to the cage-type structure in $[\{M(\text{aet})_3\}_4M''_4O]^{6+}$ ($M'' = \text{Zn}^{\text{II}}_{4-x}\text{Co}^{\text{II}}_x$) by substitution of bridging $\text{Co}(\text{III})$ for $\text{Zn}(\text{II})$.⁵ In these circumstances, it is worthwhile to investigate the reaction of $\text{fac}(\text{S})$ - $[\text{Co}(\text{aet})_3]$ with Zn^{2+} in order to elucidate the long-standing question about the $\text{Co}^{\text{III}}\text{Zn}^{\text{II}}$ S-bridged polynuclear structure.

The structural analysis presented in this work confirms that the reaction of $\text{fac}(\text{S})$ - $[\text{Co}(\text{aet})_3]$ with Zn^{2+} does not form a linear-type but a cage-type S-bridged polynuclear complex, which is spontaneously resolved (Scheme I). The crystal structure and absolute configuration of the cage-type $\text{Co}^{\text{III}}\text{Zn}^{\text{II}}$ complex, together with its spectrochemical and electrochemical properties, are reported.

Experimental Section

Synthesis. A. $\text{fac}(\text{S})$ - $[\text{Co}(\text{aet})_3]$,^{1a} $\Delta_{\text{LLL}}\text{-fac}(\text{S})\text{-K}_3[\text{Co}(\text{L-cys-N,S})_3]\cdot 9\text{H}_2\text{O}$,^{2a} and $\Delta\Delta\text{-}[\text{Co}\{\text{Co}(\text{aet})_3\}_2](\text{NO}_3)_3$ ^{2d} were prepared by the methods described in previous papers.

B. To a suspension containing 0.5 g (1.7 mmol) of $\text{fac}(\text{S})$ - $[\text{Co}(\text{aet})_3]$ in 25 cm³ of water was added a solution containing 0.7 g (3.1 mmol) of ZnBr_2 in 5 cm³ of water. The mixture was stirred at room temperature for 30 min, whereupon the suspension became a black solution. The reaction solution was filtered and to the filtrate was added 10 g of NaBr in 20 cm³ of water, followed by storing the filtrate in a refrigerator (0 °C) for 1 day. The resulting dark greenish brown precipitate (1) was collected by filtration and washed with methanol and ethanol. Yield: 0.82 g (87%). Anal. Calcd for $[\{\text{Co}(\text{aet})_3\}_4\text{Zn}_4\text{Br}_6] \cdot 7.5\text{H}_2\text{O} \cdot 2\text{NaBr}$,

- (2) (a) Konno, T.; Aizawa, S.; Okamoto, K.; Hidaka, J. *Chem. Lett.* **1985**, 1017. (b) Okamoto, K.; Aizawa, S.; Konno, T.; Einaga, H.; Hidaka, J. *Bull. Chem. Soc. Jpn.* **1986**, 59, 3859. (c) Aizawa, S.; Okamoto, K.; Einaga, H.; Hidaka, J. *Bull. Chem. Soc. Jpn.* **1988**, 61, 1601. (d) Miyawaki, S.; Konno, T.; Okamoto, K.; Hidaka, J. *Bull. Chem. Soc. Jpn.* **1988**, 61, 2987. (e) Konno, T.; Aizawa, S.; Hidaka, J. *Bull. Chem. Soc. Jpn.* **1989**, 62, 585. (f) Konno, T.; Aizawa, S.; Okamoto, K.; Hidaka, J. *Bull. Chem. Soc. Jpn.* **1990**, 63, 792.
(3) Konno, T.; Okamoto, K.; Hidaka, J. *Bull. Chem. Soc. Jpn.* **1990**, 63, 3027.
(4) Konno, T.; Okamoto, K.; Hidaka, J. *Chem. Lett.* **1990**, 1043.
(5) Konno, T.; Okamoto, K.; Hidaka, J. *Inorg. Chem.* **1991**, 30, 2253.
(6) The present authors, unpublished results.

Table I. Crystallographic Data for $[\{\text{Co}(\text{aet})_3\}_4\text{Zn}_4\text{O}]\text{Br}_6 \cdot 9.5\text{H}_2\text{O}$

chem formula	$\text{C}_{24}\text{H}_{91}\text{N}_{12}\text{S}_{12}\text{O}_{10.5}\text{Co}_4\text{Zn}_4\text{Br}_6$
fw	2077.9
space group	$P2_13$ (No. 198)
<i>a</i> , Å	18.981 (1)
<i>V</i> , Å ³	6838.6 (3)
ρ_{obsd} , g cm ⁻³	2.03
ρ_{calcd} , g cm ⁻³	2.02
<i>Z</i>	4
abs coeff, cm ⁻¹	60.8
transm coeff	0.694–0.992
temp, °C	23
λ (Mo, K α), Å	0.71069
$R(F_o)$ ^a	0.0478
$R_w(F_o)$ ^{b,c}	0.0448
$R(F_o)$ ^{d,e}	0.0612
$R_w(F_o)$ ^{b,d,e}	0.0599
$R(F_o)_2/R(F_o)_1$ ^f	1.28

^a $R(F_o) = \sum(|F_o| - |F_c|) / \sum(|F_o|)$. ^b $R_w(F_o) = (\sum w(|F_o| - |F_c|)^2) / \sum w(|F_o|)^2)^{1/2}$. ^c $w = 3.33 / (\sigma^2(F_o) + (4.9 \times 10^{-4})|F_o|^2)$. ^d $w = 3.73 / (\sigma^2(F_o) + (5.3 \times 10^{-4})|F_o|^2)$. ^e Refinement in the enantiomeric parameters. ^f Hamilton test;¹⁰ $R_{1.1604,0.005} = 1.003$.

$\text{C}_{24}\text{H}_{72}\text{N}_{12}\text{S}_{12}\text{Co}_4\text{Zn}_3\text{Br}_6 \cdot 7.5\text{H}_2\text{O} \cdot 2\text{NaBr}$: C, 13.31; H, 4.05; N, 7.76; Co, 10.88; Zn, 9.06. Found: C, 13.53; H, 4.07; N, 7.76; Co, 10.45; Zn, 9.47.

A 0.5-g sample of 1 was dissolved in a small amount of water, and the solution was allowed to stand in a refrigerator for a week. The resulting fine black crystals (2) were collected by filtration. Yield: 0.22 g (46%). Anal. Calcd for $[\{\text{Co}(\text{aet})_3\}_4\text{Zn}_4\text{O}]\text{Br}_6 \cdot 9.5\text{H}_2\text{O}$, $\text{C}_{24}\text{H}_{72}\text{N}_{12}\text{OS}_{12}\text{Co}_4\text{Zn}_4\text{Br}_6 \cdot 9.5\text{H}_2\text{O}$: C, 13.87; H, 4.41; N, 8.09; Co, 11.34; Zn, 12.56. Found: C, 13.92; H, 4.43; N, 8.00; Co, 11.14; Zn, 12.46.

2 was also prepared by the reaction of $\text{fac}(\text{S})$ - $[\text{Co}(\text{aet})_3]$ (0.5 g) and ZnBr_2 (0.7 g) in water (25 cm³) at 60 °C for 30 min, followed by cooling the mixture in a refrigerator for 1 day. Yield: 0.53 g (59%). Anal. Found: C, 13.89; H, 4.27; N, 8.04; Co, 10.99; Zn, 12.62.

Slow evaporation of an aqueous solution of 2 at room temperature afforded spontaneously resolved crystals suitable for X-ray analysis; two crystal forms which are not superimposable on each other exist, and each crystal that was picked up from the bulk showed a positive or negative CD sign with the same $|\Delta\epsilon|$ value at 580 nm.

Measurements. The electronic absorption spectra were recorded with a JASCO UVIDE-505 or UVIDE-610C spectrophotometer, and the CD spectra, with a JASCO J-600 spectropolarimeter. The concentrations of Co and Zn in the complexes were determined with a Nippon Jarrel-Ash ICPA-575 ICP spectrophotometer. The ¹³C NMR spectra were recorded with a Bruker AM-500 NMR spectrometer at the probe temperature in D₂O. Sodium 4,4-dimethyl-4-silapentane-1-sulfonate (DSS) was used as the internal reference. Electrochemical measurements were made with a CV-1B apparatus (Bioanalytical Systems, Inc.) using a glassy-carbon working electrode (Bioanalytical Systems, Inc., GCE). An aqueous $\text{Ag}/\text{AgCl}/\text{NaCl}$ (3 mol dm⁻³) electrode (Bioanalytical Systems, Inc., RE-1) and platinum wire were used as reference and auxiliary electrodes, respectively. Electrochemical experiments were conducted at 22 °C in a 0.1 mol dm⁻³ aqueous solution of NaNO_3 as the supporting electrolyte and complex concentrations of 1.0 mmol dm⁻³.

X-ray Structure Determination. A black crystal of 2 ($[\{\text{Co}(\text{aet})_3\}_4\text{Zn}_4\text{O}]\text{Br}_6 \cdot 9.5\text{H}_2\text{O}$) was mounted on a glass fiber, coated with epoxy as a precaution against solvent loss, and centered on an Enraf Nonius CAD4 diffractometer with a graphite-monochromatized Mo $K\alpha$ radiation. Unit cell parameters were determined by a least-squares refinement, using the setting angles of 25 reflections in the range of $23 < 2\theta < 26^\circ$. The systematic absences led to the choice of either the space group $P2_12_12_1$ (No. 19) or $P2_13$ (No. 198). When the structure was solved by using the space group $P2_12_12_1$, all atoms of the complex cation exist almost on the positions expected for the site symmetry of $P2_13$. Hence, the space group was deduced to be $P2_13$, and this assignment was confirmed by the eventual structure refinement. Crystallographic data are summarized in Table I. The intensity data were collected by the ω - 2θ scan mode up to $2\theta = 50^\circ$ ($+h,+k,+l$). A total of 6615 reflections were collected, 1844 of which were considered to be observed ($F_o > 5\sigma(F_o)$). Data reduction and application of Lorentz, polarization, decomposition, and empirical absorption corrections based on a series of χ scans were carried out by using the Enraf-Nonius Structure Determination Package.⁷

(7) Enraf-Nonius Structure Determination Package (SDP); Enraf-Nonius: Delft, Holland, 1978.

Table II. Final Atomic Coordinates and Equivalent Isotropic Thermal Parameters (\AA^2)

atom	x	y	z	$B_{\text{eq}}, \text{\AA}^2$	occ
CoA	0.6152 (1)	0.8952 (1)	0.8163 (1)	2.3 (1)	
S1A	0.7016 (1)	0.9383 (2)	0.7460 (2)	2.3 (1)	
S2A	0.6815 (2)	0.8923 (2)	0.9154 (2)	2.6 (1)	
S3A	0.6408 (2)	0.7820 (2)	0.7884 (2)	2.8 (1)	
N1A	0.5909 (5)	0.9963 (6)	0.8356 (6)	3.5 (5)	
N2A	0.5353 (5)	0.8630 (6)	0.8763 (5)	3.2 (5)	
N3A	0.5497 (5)	0.8937 (7)	0.7332 (6)	3.8 (5)	
C1A	0.6885 (7)	1.0325 (7)	0.7602 (8)	3.7 (6)	
C2A	0.6546 (7)	1.0444 (7)	0.8325 (8)	3.8 (7)	
C3A	0.6187 (7)	0.8412 (9)	0.9698 (7)	4.5 (7)	
C4A	0.5490 (9)	0.8595 (13)	0.9531 (8)	6.8 (11)	
C5A	0.5942 (8)	0.7782 (9)	0.7009 (9)	6.0 (9)	
C6A	0.5347 (11)	0.8244 (12)	0.7018 (12)	8.6 (13)	
CoB	0.9414 (1)	0.9414 (1)	0.9414 (1)	2.0 (1)	$1/3$
S1B	0.8562 (2)	0.9861 (2)	0.8709 (2)	2.6 (1)	
N1B	1.0035 (6)	1.0197 (5)	0.9062 (5)	3.0 (5)	
C1B	0.9051 (9)	1.0582 (8)	0.8299 (10)	5.8 (9)	
C2B	0.9773 (10)	1.0496 (11)	0.8389 (11)	7.4 (11)	
ZnA	0.8178 (1)	0.9131 (1)	0.7802 (1)	2.0 (1)	$1/3$
ZnB	0.7583 (1)	0.7583 (1)	0.7583 (1)	2.2 (1)	$1/3$
O	0.8171 (4)	0.8171 (4)	0.8171 (4)	1.8 (2)	$1/3$
Br1A	0.4991 (1)	0.5594 (2)	0.8207 (2)	6.9 (1)	0.85
Br1B	0.5131 (6)	0.5862 (8)	0.7610 (11)	7.5 (8)	0.15
Br2	0.3289 (1)	0.3289 (1)	0.3289 (1)	4.2 (1)	$1/3$
Br3A	0.5421 (2)	0.5421 (2)	0.5421 (2)	5.3 (2)	$2/9$
Br3B	0.5215 (5)	0.5215 (5)	0.5215 (5)	5.3 (4)	$1/9$
Br4A	-0.6641 (3)	-0.1641 (3)	0.6641 (3)	10.5 (3)	$2/9$
Br4B	0.3331 (18)	0.8195 (23)	0.6174 (13)	13.8 (22)	$1/9$
O1W	0.4285 (10)	0.6957 (8)	0.5929 (7)	10.4 (10)	
O2W	0.6645 (9)	0.2242 (11)	0.6948 (11)	12.7 (13)	
O3W	0.4715 (8)	0.7217 (9)	0.8630 (8)	9.4 (9)	
O4W	-0.5666 (12)	-0.0666 (12)	0.5666 (12)	8.8 (22)	$1/6$

$^a B_{\text{eq}}$ is the arithmetic mean of the principal axes of the thermal ellipsoid.

The structure for the space group $P2_12_12_1$ was solved by direct method⁷ and conventional difference Fourier techniques. The structure for the space group $P2_13$ was solved by using the non-hydrogen atom positions of one-third of the formula unit obtained from the space group $P2_12_12_1$. The CoB, ZnB, and O atoms in the complex cation, four Br atoms (Br2, Br3A, Br3B, Br4A), and one O atom of the water molecule (O4W) were constrained to the special positions of symmetry 3. Three of the four independent Br atoms (Br1, Br3, Br4) exhibited positional disorder and were best modeled with two positions for each atom. The structure was refined by full-matrix least-squares techniques using SHELX76.⁸ All non-hydrogen atoms were refined anisotropically, and hydrogen atoms were not included in the calculation. Scattering factors and anomalous dispersion corrections for Co and Zn were taken from ref 9, while all others were supplied in SHELX76. Non-hydrogen atom coordinates are listed in Table II. Listings of anisotropic thermal parameters and observed and calculated structure factors have been deposited as supplementary material.

Results and Discussion

Crystal Structure of (+)₅₈₀^{CD}-[[Co(aet)₃]₄ZnO]Br₆ (2). X-ray structural analysis of **2**, which showed a positive CD value at 580 nm, revealed the presence of a discrete complex cation, bromide anions, and water molecules. There are four crystallographically independent bromide anions, three of which (Br1, Br3, and Br4) exhibited positional disorder (Table II). The total site occupancy factor of the bromide anions implies that the entire complex cation is hexavalent. Perspective drawings of the entire complex cation are given in parts a and b of Figure 1, and the polyhedral representation of the complex cation is depicted in Figure 2. The bond lengths and angles in the complex cation are listed in Table III.

The entire complex cation has crystallographically imposed C_3 symmetry, the CoB, O, and ZnB atoms lying on the 3-fold axis.

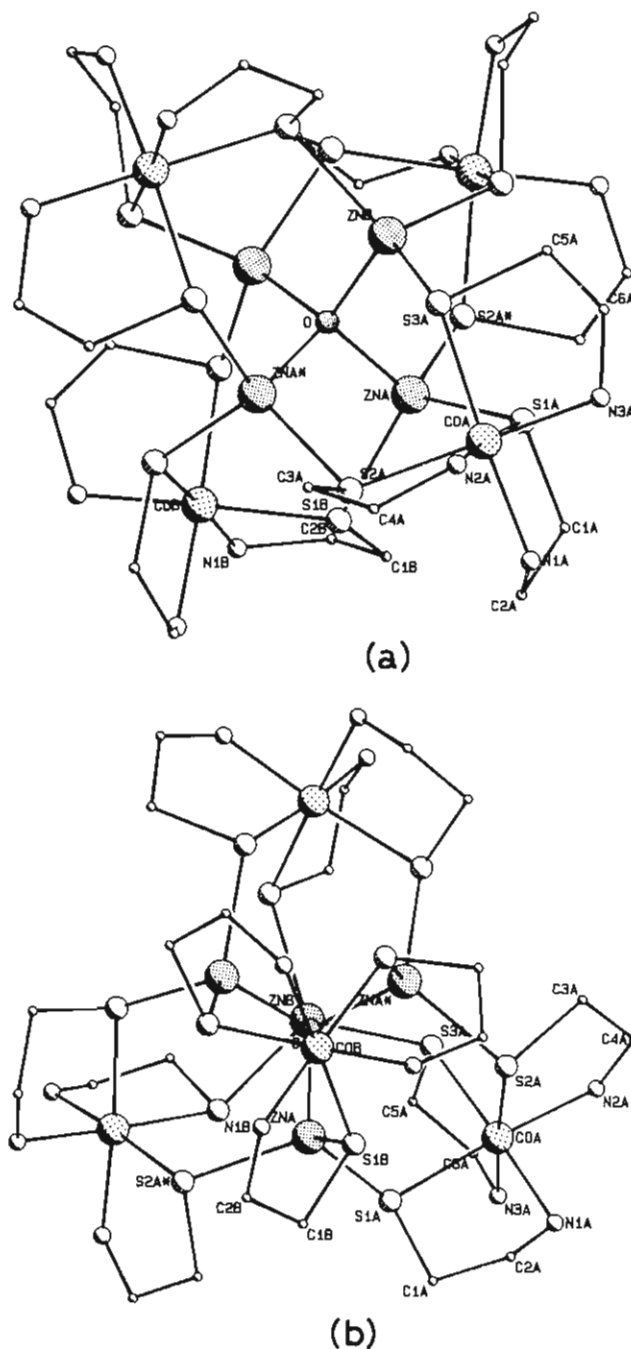


Figure 1. Perspective views of the complex cation of **2** with the atomic labeling scheme: (a) view down an axis close to a C_2 axis; (b) view down an axis close to a C_3 axis.

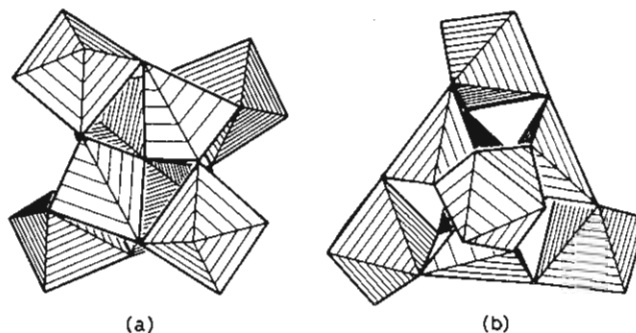


Figure 2. Polyhedral representation of the complex cation of **2**: (a) view down an axis close to a C_2 axis; (b) view down an axis close to a C_3 axis.

As shown in Figure 1a,b, the complex cation consists of four approximately octahedral $\text{fac}(S)\text{-[Co(aet)}_3\text{]}$ subunits, four zinc

(8) Sheldrick, G. M. *SHELX76, A Program for X-ray Crystal Structure Determination*; University of Cambridge: Cambridge, U.K., 1976.

(9) Cromer, D. T.; Waber, J. T. *International Tables for X-ray Crystallography*; Kynoch Press: Birmingham, U.K., 1974; Vol. IV.

Table III. Bond Distances (Å) and Angles (deg)

CoA-S1A	2.267 (3)	N3A-C6A	1.472 (22)
CoA-S2A	2.264 (3)	C1A-C2A	1.533 (19)
CoA-S3A	2.266 (4)	C3A-C4A	1.404 (22)
CoA-N1A	2.007 (11)	C5A-C6A	1.430 (24)
CoA-N2A	1.992 (10)	CoB-S1B	2.266 (3)
CoA-N3A	2.008 (11)	CoB-N1B	2.010 (10)
S1A-C1A	1.826 (13)	S1B-C1B	1.828 (14)
S1A-ZnA	2.349 (3)	S1B-ZnA	2.327 (3)
S2A-C3A	1.851 (13)	N1B-C2B	1.484 (20)
S3A-C5A	1.883 (16)	C1B-C2B	1.390 (25)
S3A-ZnB	2.345 (3)	ZnA-O	1.953 (4)
N1A-C2A	1.515 (17)	ZnB-O	1.933 (12)
N2A-C4A	1.484 (18)		
S1A-CoA-S2A	95.5 (1)	CoA-N3A-C6A	116.7 (10)
S1A-CoA-S3A	92.8 (1)	S1A-C1A-C2A	109.5 (9)
S2A-CoA-S3A	93.0 (1)	N1A-C2A-C1A	106.3 (12)
S1A-CoA-N1A	85.9 (3)	S2A-C3A-C4A	110.5 (12)
S2A-CoA-N1A	89.9 (3)	N2A-C4A-C3A	113.5 (14)
S3A-CoA-N1A	176.9 (4)	S3A-C5A-C6A	109.7 (12)
S1A-CoA-N2A	176.1 (3)	N3A-C6A-C5A	113.6 (15)
S2A-CoA-N2A	86.6 (3)	S1B-CoB-N1B	86.9 (3)
S3A-CoA-N2A	90.3 (3)	CoB-S1B-C1B	99.7 (5)
N1A-CoA-N2A	90.8 (4)	CoB-S1B-ZnA	116.0 (1)
S1A-CoA-N3A	89.4 (3)	C1B-S1B-ZnA	106.9 (6)
S2A-CoA-N3A	175.0 (3)	S1B-CoB-S1B	93.8 (1)
S3A-CoA-N3A	86.3 (4)	CoB-N1B-C2B	111.9 (9)
N1A-CoA-N3A	90.9 (5)	N1B-CoB-N1B	90.4 (4)
N2A-CoA-N3A	88.5 (4)	S1B-C1B-C2B	111.1 (11)
CoA-S1A-C1A	99.6 (4)	N1B-C2B-C1B	118.7 (14)
CoA-S1A-ZnA	116.3 (1)	S1A-ZnA-S1B	112.2 (1)
C1A-S1A-ZnA	106.6 (5)	S1A-ZnA-O	106.4 (3)
CoA-S2A-C3A	96.8 (5)	S1B-ZnA-O	107.0 (3)
CoA-S3A-C5A	98.1 (5)	ZnA-O-ZnA	109.3 (3)
CoA-S3A-ZnB	116.3 (1)	S3A-ZnB-O	107.3 (1)
C5A-S3A-ZnB	102.9 (5)	ZnA-O-ZnB	109.6 (3)
S3A-ZnB-S3A	111.6 (1)		
CoA-N1A-C2A	112.7 (7)		
CoA-N2A-C4A	116.2 (10)		

atoms, and one central μ_4 -oxygen atom. This is consistent with that the plasma emission spectral analysis gave the value of Co:Zn = 4:4 in **2**. The four zinc atoms are bound to the central oxygen atom in a tetrahedral geometry (ZnA-O-ZnA = 109.3 (3)°, ZnA-O-ZnB = 109.6 (3)°, ZnA-O = 1.953 (4) Å, ZnB-O = 1.933 (12) Å), and to this tetrahedral [Zn₄O]⁶⁺ core (ZnA-ZnA-ZnA = 60.00 (4)°, ZnA-ZnA-ZnB = 59.90 (4)°, ZnA-ZnB-ZnA = 60.19 (4)°) are bound the four *fac*(S)-[Co(aet)₃] subunits in a tetrahedral arrangement (CoA-CoA-CoA = 60.00 (2)°, CoA-CoA-CoB = 59.90 (2)°, CoA-CoB-CoA = 60.23 (2)°), completing the cage-type S-bridged octanuclear structure. The Zn...Zn and Zn...Co distances fall in the ranges 3.177 (2)–3.186 (2) Å and 3.895 (2)–3.921 (2) Å, respectively, indicating that no direct metal-metal interaction exists in [(Co(aet)₃)₄Zn₄O]⁶⁺. In the present S-bridged octanuclear complex, each zinc atom is situated in an approximately tetrahedral environment, coordinated by three sulfur atoms from three different *fac*(S)-[Co(aet)₃] subunits and an oxygen atom at the center of the polynuclear structure (S1A-ZnA-S1B = 112.2 (1)°, S1A-ZnA-O = 106.4 (3)°, S1B-ZnA-O = 107.0 (3)°, S3A-ZnB-S3A = 111.6 (1)°, S3A-ZnB-O = 107.3 (1)°; ZnA-S1A = 2.349 (3) Å, ZnB-S3A = 2.345 (3) Å, ZnA-S1B = 2.327 (3) Å). This is in contrast to the central metal ion (M' = Fe(III), Co(III), Ni(II)) being octahedrally coordinated by six sulfur atoms from two terminal *fac*(S)-[M(aet or L-cys-N,S)₃]^{0 or 3-} (M = Co(III), Rh(III), Ir(III)) in the linear-type S-bridged trinuclear structure, [M{M(aet or L-cys-N,S)₃}]^{n+ or n-1,2}.

The complex cation has two kinds of chiral centers, Δ or Λ for the *fac*(S)-[Co(aet)₃] subunits and *R* or *S* for the bridging sulfur atoms. The absolute configurations for the spontaneously resolved (+)₅₈₀^{CD} isomer was determined by the anomalous scattering technique. The structure containing the Λ configuration of *fac*(S)-[Co(aet)₃] subunits in the complex cation is probably the correct choice, and its enantiomeric structure could be rejected at the 0.005 significance level by the Hamilton test (Table I).¹⁰

Thus, all four *fac*(S)-[Co(aet)₃] subunits take Λ and all 12 bridging sulfur atoms take *R* in (+)₅₈₀^{CD}[(Co(aet)₃)₄Zn₄O]⁶⁺, as shown in Figure 1a,b. All 12 five-membered aet chelate rings take the reasonable gauche form with a δ conformation.

The bond lengths associated with the aet ligands (average S-C = 1.847 (16) Å, C-C = 1.439 (25) Å, and C-N = 1.489 (22) Å) are within the range normally observed for the aet metal complexes.^{10,11,12} The Co-N bond lengths (average 2.004 (11) Å) are in good agreement with those found in the linear-type S-bridged tricobalt(III) complex [CoCo(aet)₃]³⁺ (average 1.996 (8) Å), while the Co-S bond lengths (average 2.266 (4) Å) are somewhat longer than those in [CoCo(aet)₃]³⁺ (average = 2.238 (7) Å).¹⁰ The N-Co-N bond angles (average 90.2 (5)°) are normal and similar to those in the mononuclear *fac*(S)-[Co(2-aminoethanesulfenato-N,S)₃] complex (average 90.7 (5)°).¹³ However, the S₃ faces are expanded to give the obtuse S-Co-S angles (average 93.8 (1)°), compared with the normal S-Co-S angles observed in *fac*(S)-[Co(2-aminoethanesulfenato-N,S)₃] (average 89.4 (1)°). This is in contrast to the fact that all S-Co-S angles are acute (average 84.5 (8)°) and all N-Co-N angles are obtuse (average 94.6 (6)°) in [CoCo(aet)₃]³⁺.¹⁰

Several hydrogen bonds between amine groups and water molecules exist within the unit cell; the distances of N2A...O1W, N2A...O3W, and N3A...O1W are 3.055 (18), 2.954 (20), and 3.096 (18) Å, respectively.

Synthesis and Properties. The reaction of *fac*(S)-[Co(aet)₃] with ZnBr₂ in water at room temperature, followed by the addition of a large amount of NaBr, gave a dark greenish brown precipitate (**1**). Recrystallization of **1** from water resulted in the formation of the cage-type S-bridged octanuclear complex with a "complete" core [Zn₄O]⁶⁺, [(Co(aet)₃)₄Zn₄O]⁶⁺ (cation of **2**), which is spontaneously resolved. **2** can also be prepared by the reaction of *fac*(S)-[Co(aet)₃] with Zn²⁺ in water at a high temperature (ca. 60 °C). The analogous cage-type S-bridged octanuclear complexes with a "complete" core, [(M(aet)₃)₄M'₄O]⁶⁺ (M = Rh^{III}, Ir^{III}; M' = Zn^{II}, Co^{II}), which are spontaneously resolved, have been prepared from the reaction of the linear-type S-bridged trinuclear complexes [Co^{III}{M(aet)₃}]³⁺ and Zn powder in water.⁵ **2** is fairly stable in water as in the case of [(M(aet)₃)₄M'₄O]⁶⁺; no significant electronic absorption and CD spectral changes with time were noticed for several hours.

Two optical isomers of **2**, (+)₅₈₀^{CD} and (-)₅₈₀^{CD}, which were spontaneously resolved, show CD spectra enantiomeric to each other. Since the (+)₅₈₀^{CD} isomer was determined by X-ray crystallography to take the Λ configuration for all the four *fac*(S)-[Co(aet)₃] subunits, the (-)₅₈₀^{CD} isomer can be assigned to take the $\Delta\Delta\Delta\Delta$ configuration. Molecular model constructions reveal that a significant nonbonding interaction comes into exist among the aet chelate rings of adjacent *fac*(S)-[Co(aet)₃] subunits when the absolute configuration of the four subunits is not uniform. Accordingly, either of the Δ or Λ isomer of *fac*(S)-[Co(aet)₃] is selectively incorporated in [(Co(aet)₃)₄Zn₄O]⁶⁺, forming only the $\Delta\Delta\Delta\Delta$ and $\Lambda\Lambda\Lambda\Lambda$ isomers with an approximate *T* symmetry. The ¹³C NMR spectrum of **2** in D₂O shows only two signals due to two kinds of methylene carbon atoms of the aet ligand (δ 34.21 for -CH₂S and δ 50.41 for -CH₂NH₂ from DSS), suggesting that the *T* symmetrical structure observed in the crystal is retained in solution.

Figure 3 illustrates the visible-UV absorption and CD spectra of the present cage-type complex (-)₅₈₀^{CD}- $\Delta\Delta\Delta\Delta$ -[(Co(aet)₃)₄Zn₄O]⁶⁺ (cation of **2**) and the linear-type complex $\Delta\Delta$ -[CoCo(aet)₃]³⁺, together with those of *fac*(S)-[Co(aet)₃] and Δ_{LLL} -*fac*(S)-[Co(L-cys-N,S)₃]³⁻; the data are summarized in Table IV. **2** exhibits two d-d transition bands (ca. 18 × 10³ and 24 × 10³ cm⁻¹) in the visible region and two intense sulfur-to-cobalt charge-transfer (CT) bands (ca. 30 × 10³ and 38 × 10³ cm⁻¹)

(10) Hamilton, W. C. *Acta Crystallogr.* 1965, 18, 502.(11) Elder, R. C.; Florian, L. R.; Lake, R. E.; Yacynych, A. M. *Inorg. Chem.* 1973, 12, 2690.(12) Wei, C. H.; Dahl, L. F. *Inorg. Chem.* 1970, 9, 1878.(13) Kita, M.; Yamanari, K.; Kitahara, K.; Shimura, Y. *Bull. Chem. Soc. Jpn.* 1981, 54, 2995.

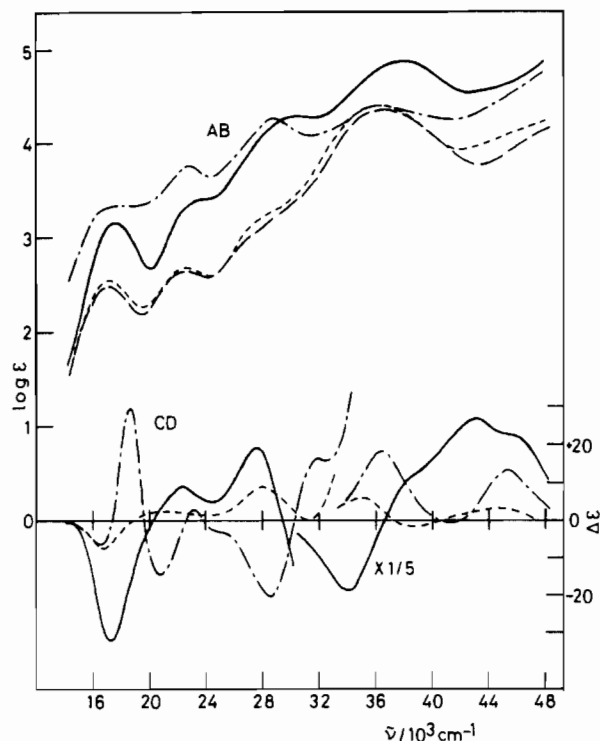


Figure 3. Visible-UV absorption and CD spectra of $\Delta\Delta\Delta\Delta$ -[Co(aet)₃]₄Zn₄O]⁶⁺ (cation of **2**) (—), *fac*(S)-[Co(aet)₃] (---), Δ_{LLL} -*fac*(S)-[Co(L-cys-*N,S*)₃]³⁻ (---), and $\Delta\Delta$ -[CoCo(aet)₃]₂³⁺ (---) in H₂O. ϵ values are given in units of mol⁻¹ dm³ cm⁻¹.

Table IV. Visible-UV Absorption and CD Spectral Data^a

complex	abs max $\bar{\nu}/10^3 \text{ cm}^{-1}$ (log ϵ)	CD extrema $\bar{\nu}/10^3 \text{ cm}^{-1}$ ($\Delta\epsilon/\text{mol}^{-1} \text{ dm}^3 \text{ cm}^{-1}$)
[Co(aet) ₃] ₄ Zn ₃ Br] ⁵⁺	17.86 (3.16)	
	23.8 (3.5 sh)	
	30.1 (4.2 sh)	
	37.59 (4.79)	
$(-)^{CD}_{580}$ - $\Delta\Delta\Delta\Delta$ -[Co(aet) ₃] ₄ Zn ₄ O] ⁶⁺	17.67 (3.16)	17.15 (-32.41)
	23.9 (3.4 sh)	22.08 (+8.81)
	30.6 (4.3 sh)	27.17 (+19.07)
	38.02 (4.87)	33.67 (-94.42)
		41.84 (+134.6)
<i>fac</i> (S)-[Co(aet) ₃]	17.15 (2.49)	
	22.57 (2.65)	
	28.3 (3.2 sh)	
	36.50 (4.35)	
Δ_{LLL} - <i>fac</i> (S)-[Co(L-cys- <i>N,S</i>) ₃] ³⁻	17.18 (2.54)	16.72 (-7.53)
	22.62 (2.68)	20.83 (+2.06)
	28.9 (3.3 sh)	28.17 (+8.60)
	34.96 (4.39)	34.96 (+28.30)
		38.61 (-9.43)
$\Delta\Delta$ -[CoCo(aet) ₃] ₂ ³⁺	18.35 (3.34)	16.53 (-6.45)
	22.73 (3.76)	18.62 (+29.76)
	28.82 (4.26)	20.79 (-14.39)
	36.23 (4.40)	23.15 (+3.00)
		25.1 (-3.2 sh)
		28.65 (-20.34)
		31.85 (+16.12)
		36.36 (+90.52)
		42.32 (-3.72)
		45.25 (+65.72)

^a The sh label denotes a shoulder.

in the near-UV region, in accordance with the absorption spectral data obtained by Douglas et al.^{1b} This absorption spectral feature is similar to that of *fac*(S)-[Co(aet or L-cys-*N,S*)₃]^{0 or 3-}, and furthermore, the absorption curve coincides with that of 4 mol of *fac*(S)-[Co(aet or L-cys-*N,S*)₃]^{0 or 3-} over the whole region (Figure 4). This indicates that the absorption spectrum of **2** is dominated by the four *fac*(S)-[Co(aet)₃] subunits, that is, the electronic state of facially coordinated sulfur atoms of [Co(aet)₃]

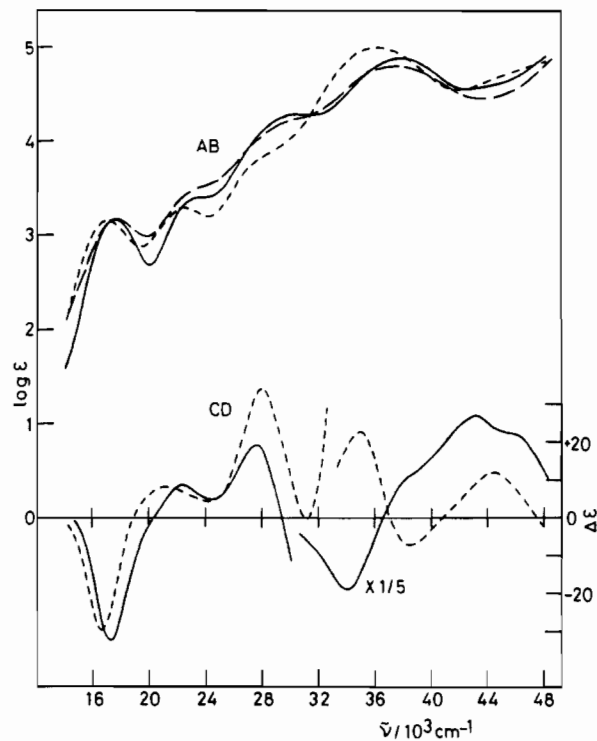


Figure 4. Visible-UV absorption and CD spectra of $\Delta\Delta\Delta\Delta$ -[Co(aet)₃]₄Zn₄O]⁶⁺ (cation of **2**) (—), Δ_{LLL} -*fac*(S)-[Co(L-cys-*N,S*)₃]³⁻ ($\times 4$) (---), and [Co(aet)₃]₄Zn₃Br]⁵⁺ (cation of **1**) (---). ϵ values are given in units of mol⁻¹ dm³ cm⁻¹.

is little affected by bridging with Zn(II). On the other hand, the absorption spectrum of [CoCo(aet)₃]₂³⁺ is markedly intensified in the region of (16–30) $\times 10^3 \text{ cm}^{-1}$ compared with that of *fac*(S)-[Co(aet or L-cys-*N,S*)₃]^{0 or 3-}, although their CT bands at ca. $36 \times 10^3 \text{ cm}^{-1}$ coincide well each other. This spectral deviation can be ascribed to the contribution due to the central CoS₆ chromophore in the linear-type [CoCo(aet)₃]₂³⁺.

Two kinds of CD contributions are expected for $(-)^{CD}_{580}$ - $\Delta\Delta\Delta\Delta$ -[Co(aet)₃]₄Zn₄O]⁶⁺ (cation of **2**), one from four Δ -*fac*(S)-[Co(aet)₃] subunits and the other from 12 S configurational sulfur atoms; both contributions can not be separated. The CD spectrum of **2** is quite similar to that of 4 mol of Δ_{LLL} -*fac*(S)-[Co(L-cys-*N,S*)₃]³⁻ in the region of (16–30) $\times 10^3 \text{ cm}^{-1}$, as in the case of their absorption spectral behavior (Figure 4). This good agreement suggests that for the present cage-type S-bridged complex **2** the CD contribution due to asymmetric sulfur atoms is minor in this region. Therefore, the absolute configuration of the cage-type S-bridged Co^{III}Zn^{II} complex can be assigned by comparing the CD spectral pattern with Δ_{LLL} -*fac*(S)-[Co(L-cys-*N,S*)₃]³⁻ in this region. In the near-UV region ((30–48) $\times 10^3 \text{ cm}^{-1}$), however, the CD spectral behavior of **2** differs significantly from that of 4 mol of Δ_{LLL} -*fac*(S)-[Co(L-cys-*N,S*)₃]³⁻ (Figure 4). In particular, the CD bands of **2** in the sulfur-to-cobalt CT band region ((32–40) $\times 10^3 \text{ cm}^{-1}$) are reversed in sign compared with those of 4 mol of Δ_{LLL} -*fac*(S)-[Co(L-cys-*N,S*)₃]³⁻. Taking into consideration that the L-cys-*N,S*-cobalt(III) complexes commonly show CD spectral patterns similar to the corresponding aet complexes,^{1b,2,14,15} in other word, the vicinal CD contribution due to L-cys-*N,S* ligands is relatively small, it is reasonable to assume that the S configurational sulfur atoms contribute dominantly to the CD spectra in the sulfur-to-cobalt CT band region. Contrary to the cage-type S-bridged complex **2**, the CD spectral pattern of $\Delta\Delta$ -[CoCo(aet)₃]₂³⁺ differs remarkably from that of Δ_{LLL} -*fac*(S)-[Co(L-cys-*N,S*)₃]³⁻ in the region (16–30) $\times 10^3 \text{ cm}^{-1}$, while they show CD spectral patterns similar to each other in the

(14) Freeman, H. C.; Moore, C. J.; Jackson, W. G.; Sargeson, A. M. *Inorg. Chem.* **1978**, *17*, 3513.

(15) Konno, T.; Okamoto, K.; Hidaka, J. *Bull. Chem. Soc. Jpn.* **1984**, *57*, 3104.

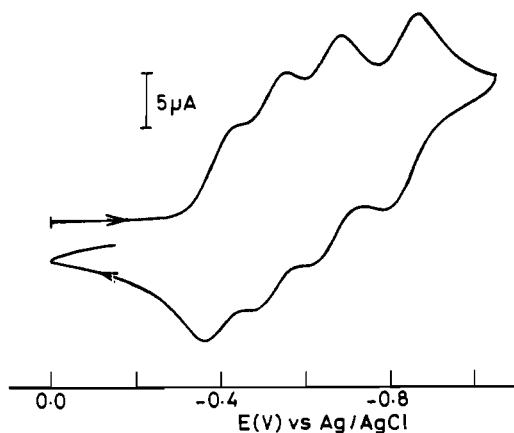
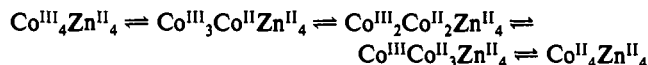


Figure 5. Cyclic voltammogram of 1.0 mmol dm⁻³ [Co(aet)₃]₄Zn₄O⁶⁺ (cation of 2) in 0.1 mol dm⁻³ aqueous solution of NaNO₃. The scan rate is 50 mV s⁻¹.

region (32–48) × 10³ cm⁻¹ (Figure 3). This CD spectral deviation suggests that the asymmetric bridging sulfur atoms of the central CoS₆ chromophore in ΔΔ-[Co{Co(aet)₃}₂]³⁺ contribute conspicuously to the CD spectrum in the region (16–30) × 10³ cm⁻¹.

Electrochemical experiments were performed in a 0.1 mol dm⁻³ NaNO₃ aqueous solution at a glassy carbon electrode. As shown in Figure 5, the cyclic voltammogram of [Co(aet)₃]₄Zn₄O⁶⁺ (2) initiated at 0.0 V with a negative potential scan yields four consecutive reduction waves ($E_{pc} = -0.44, -0.56, -0.69, -0.87$ V) and coupled four oxidation waves ($E_{pa} = -0.36, -0.48, -0.61, \text{ and } -0.79$ V). No other redox couple is observed in the potential region of +0.8 to -1.2 V (vs Ag/AgCl). The peak current is approximately proportional to the square root of the scan rate. At a scan rate of 50 mV s⁻¹, the ratio of cathodic to anodic peak current is approximately unity and the observed peak separation ($E_{pc} - E_{pa}$)

is 80 mV for each redox couple. These results establish that the four redox processes which occur at $E^{\circ} = -0.40, -0.52, -0.65,$ and -0.83 V are electrochemically quasi-reversible. For the corresponding Rh^{III}Zn^{II} complexes, [Rh(aet)₃]₄Zn₃O⁴⁺ and [Rh(aet)₃]₄Zn₄O⁶⁺,^{4,5} no redox reaction has occurred in the region of +0.8 to -1.2 V under the same condition. Therefore, the four redox processes can be assigned as the stepwise reactions as follows:



In order to estimate the structure of 1, its cyclic voltammetric measurement was performed under the same conditions as used for 2. The cyclic voltammogram of 1 gave broad and nonreversible four consecutive reduction waves at $E_{pc} = -0.45, -0.57, -0.71,$ and -0.89 V. This electrochemical behavior analogies with that of 2, although the relative instability of 1 in water restricts the electrochemical characterization. In addition, the absorption spectrum of 1 is quite similar to that of 2 over the whole region, as shown in Figure 4. These facts suggest that 1 has a cage-type S-bridged structure similar to that of 2. The plasma emission spectral analysis indicates that 1 contains Co and Zn in a ratio of 4:3. Accordingly, it is likely that 1 is the cage-type S-bridged complex with a "defective" [Zn₃Br]⁵⁺ core, [Co(aet)₃]₄Zn₃Br]⁵⁺, considering that the formation of 1 was achieved by the addition of a large amount of NaBr to the reaction solution of *fac*(S)-[Co(aet)₃] and Zn²⁺.

Registry No. 1, 139100-76-8; 2-Br₆ (Δ-isomer), 139100-77-9; 2-Br₆·9.5H₂O (Δ-isomer), 139236-12-7; 2⁶⁺ (Δ-isomer), 139236-13-8; *fac*(S)-[Co(aet)₃], 18703-22-5; ΔΔ-[Co{Co(aet)₃}₂](NO₃)₃, 129387-95-7; Δ_{LLL}-*fac*(S)-K₃[Co(L-cys-N,S)₃], 97860-43-0.

Supplementary Material Available: Table SI, listing anisotropic thermal parameters (1 page); Table SII, listing observed and calculated structure factors (8 pages). Ordering information is given on any current masthead page.

Contribution from the Department of Chemistry, National Taiwan University, Taipei, Taiwan, ROC

Synthesis and Characterization of Pillared Buserite

She-Tin Wong and Soofin Cheng*

Received July 19, 1991

Synthetic Na-buserite, a layered manganese oxide formulated as Na₄Mn₁₄O₂₆·xH₂O, was pillared with polyoxo cations of aluminum known widely as Keggin ions, [Al₁₃O₄(OH)₂₄(H₂O)₁₂]⁷⁺, with a diameter of 8.6 Å. The synthetic Na-buserite was first expanded with *n*-hexylammonium cations to produce hexylammonium ion-expanded buserite. This process expands the buserite interlayer free spacing from 1.94 to 12.94 Å, thus allowing subsequent ion-exchange reaction with Keggin ions to proceed. The presence of pillars between the interlayers of the buserite structure was confirmed by X-ray diffraction, thermogravimetric analysis, and surface area measurements. N₂ adsorption-desorption studies showed that the Keggin ion-pillared buserites are microporous in nature. Particular interest was focused on the studies of the thermal stability of the various materials in different gaseous environment. By complementary studies between X-ray diffraction and thermogravimetric analysis, the intermediates and the final products of these reactions can be identified.

Introduction

In the search and development of new and more efficient catalysts for use in the petroleum-related industry in particular, pillared compounds have gradually emerged as an important potential alternative to the presently available industrial catalysts.^{1,2} Among the available layered compounds, pillared clays have received the most attention and seem to have great potential in the area of acid catalysis such as cracking.^{1,3} On the other hand, the pillared derivatives of layered metal oxides, such as double hydroxide,^{4,5} Li₂MoO₃,⁶ and K₂Ti₄O₉,⁷ etc., although receiving

relatively less attention than pillared clays, have great potential to be important catalytic materials.

Most Mn oxides can be produced by a variety of pathways, and interconversions between different oxides form an important feature of this class of compounds.⁸ Birnessite, which is a partially dehydrated form of buserite, is widely distributed in soils and sediments. It is one of the important components of manganese

(1) Figueras, F. *Catal. Rev.-Sci. Eng.* **1988**, *30*, 457.
(2) Nitta, M. *Appl. Catal.* **1984**, *9*, 151.
(3) Vaughan, D. E. W. *Catal. Today* **1988**, *2*, 187.

(4) Drezdson, M. A. *Inorg. Chem.* **1988**, *27*, 4628.
(5) Pinnavaia, T. J.; Kwon, T.; Tsigdinos, G. A. *J. Am. Chem. Soc.* **1988**, *110*, 3653.
(6) Nazar, L. F.; Liblong, S. W.; Yin, X. T. *J. Am. Chem. Soc.* **1991**, *113*, 5889.
(7) Cheng, S.; Wang, T. C. *Inorg. Chem.* **1989**, *28*, 1283.
(8) Giovanoli, R. *Chimia* **1976**, *30*, 102.